Environmental Toxicology and Chemistry—Volume 00, Number 00—pp. 1–14, 2023
Received: 3 May 2023 | Revised: 24 August 2023 | Accepted: 25 October 2023

Environmental Chemistry

Effect-Directed Analysis Based on Transthyretin Binding Activity of Per- and Polyfluoroalkyl Substances in a Contaminated Sediment Extract

Håkon A. Langberg,[a,*] Sarah Choyke,[b,c] Sarah E. Hale,[a,d] Jacco Koekkoek,[e] Peter H. Cenijn,[e] Marja H. Lamoree,[e] Thomas Rundberget,[f] Morten Jartun,[f] Gijs D. Breedveld,[a,g] Bjørn M. Jenssen,[g,h] Christopher P. Higgins,[b] and Timo Hamers[e]

[a]Environment and Geotechnics, Norwegian Geotechnical Institute, Oslo, Norway
[b]Department of Civil and Environmental Engineering, Colorado School of Mines, Golden, Colorado, USA
[c]Eurofins Environment Testing, Tacoma, Washington, USA
[d]DVGW-Technologiezentrum Wasser (German Water Centre), Karlsruhe, Germany
[e]Amsterdam Institute for Life and Environment, Vrije Universiteit, Amsterdam, The Netherlands
[f]Norwegian Institute for Water Research, Oslo, Norway
[g]Department of Arctic Technology, University Centre in Svalbard, Longyearbyen, Norway
[h]Department of Biology, Norwegian University of Science and Technology, Trondheim, Norway

Abstract: Only a fraction of the total number of per- and polyfluoroalkyl substances (PFAS) are monitored on a routine basis using targeted chemical analyses. We report on an approach toward identifying bioactive substances in environmental samples using effect-directed analysis by combining toxicity testing, targeted chemical analyses, and suspect screening. PFAS compete with the thyroid hormone thyroxin (T_4) for binding to its distributor protein transthyretin (TTR). Therefore, a TTR-binding bioassay was used to prioritize unknown features for chemical identification in a PFAS-contaminated sediment sample collected downstream of a factory producing PFAS-coated paper. First, the TTR-binding potencies of 31 analytical PFAS standards were determined. Potencies varied between PFAS depending on carbon chain length, functional group, and, for precursors to perfluoroalkyl sulfonic acids (PFSA), the size or number of atoms in the group(s) attached to the nitrogen. The most potent PFAS were the seven- and eight-carbon PFSA, perfluoroheptane sulfonic acid (PFHpS) and perfluorooctane sulfonic acid (PFOS), and the eight-carbon perfluoroalkyl carboxylic acid (PFCA), perfluorooctanoic acid (PFOA), which showed approximately four- and five-times weaker potencies, respectively, compared with the native ligand T_4. For some of the other PFAS tested, TTR-binding potencies were weak or not observed at all. For the environmental sediment sample, not all of the bioactivity observed in the TTR-binding assay could be assigned to the PFAS quantified using targeted chemical analyses. Therefore, suspect screening was applied to the retention times corresponding to observed TTR binding, and five candidates were identified. Targeted analyses showed that the sediment was dominated by the di-substituted phosphate ester of N-ethyl perfluorooctane sulfonamido ethanol (SAmPAP diester), whereas it was not bioactive in the assay. SAmPAP diester has the potential for (bio)transformation into smaller PFAS, including PFOS. Therefore, when it comes to TTR binding, the hazard associated with this substance is likely through (bio)transformation into more potent transformation products. *Environ Toxicol Chem* 2023;00:1–14. © 2023 The Authors. *Environmental Toxicology and Chemistry* published by Wiley Periodicals LLC on behalf of SETAC.

Keywords: Per- and polyfluoroalkyl substances; Toxicant identification; Bioassay-directed fractionation; Endocrine disruptors

INTRODUCTION

Per- and polyfluoroalkyl substances (PFAS) are a large group of man-made chemicals (Wang et al., 2017). More than 3000 PFAS have been estimated to be on the global market (Swedish Chemicals Agency, 2015), and more than 200 use categories have been reported (Glüge et al., 2020). Some PFAS have been reported to be harmful for the environment and

This article includes online-only Supporting Information.

* Address correspondence to hakon.austad.langberg@ngi.no
Published online 27 October 2023 in Wiley Online Library (wileyonlinelibrary.com).
DOI: 10.1002/etc.5777

human health (McCarthy et al., 2017; Sunderland et al., 2019), and it has been argued that environmental contamination by PFAS has exceeded a planetary boundary (Cousins et al., 2022). Elevated PFAS exposure has been shown, or suspected, to be associated with a range of human health effects including disturbed immune function, dyslipidemia, cancer, neurodevelopmental effects, and metabolic and endocrine disruption, including disturbed thyroid system function (Sunderland et al., 2019). Associations between increased PFAS serum concentrations in humans and disturbed thyroid system functioning have been reported, including changes in thyroid-stimulating hormone and total levels of the thyroid hormone thyroxin (T_4; Blake et al., 2018). PFAS have been reported to compete with T_4 for binding to the thyroid hormone distributor protein transthyretin (TTR; Hamers et al., 2020; Weiss et al., 2009). This protein plays an important role in the delivery of T_4 to the target tissue (Richardson, 2007), and in crossing important barriers, such as the placenta (Landers & Richard, 2017) and the blood–cerebrospinal fluid barrier (Richardson et al., 2015). Deficiency of T_4 has been hypothesized to be involved in negative neurodevelopmental effects (Korevaar et al., 2016; Taheri et al., 2018).

Because different PFAS have been used for different purposes and at different times, environmental PFAS profiles (i.e., distribution profiles) vary depending on the source (Langberg et al., 2022). However, only a few PFAS are routinely monitored using targeted chemical analyses, and it is practically impossible to target all relevant PFAS in the environment. One approach for tackling the vast number of potentially harmful substances in the environment is the use of effect-directed analysis (EDA), whereby analysis efforts are focused specifically on substances showing bioactivity in bioassays indicative of specific toxicological mechanisms that may lead to adverse effects. High-throughput EDA by fractionation into microtiter plates followed by direct testing and compound identification has previously been reported (Zwart et al., 2020).

The goal of the present study was to identify unknown bioactive PFAS in a polluted environmental sediment sample. The pollution arose from a factory producing PFAS-coated paper products (Langberg et al., 2021). It has previously been reported that the pollution consists of a range of unknown fluorinated substances (Langberg et al., 2020). Because inhibition of T_4 binding to TTR through competitive binding has been suggested as one mechanism for PFAS toxicity, the TTR-binding assay was chosen for identifying bioactive PFAS. Our hypothesis was that part of the overall potency for T_4 displacement in the sample that was not explained by PFAS identified by the targeted analyses might be attributed to other, unknown PFAS. We further hypothesized that EDA would make it possible to efficiently identify these unknown bioactive PFAS.

The specific objectives of our study were as follows: 1) to test standards of 31 PFAS in the TTR-binding assay to determine TTR-binding potencies for the individual PFAS; 2) to extract sediments and fractionate sediment extract using liquid chromatography (LC); 3) to test unfractionated sediment extract as well as the different fractions of the fractionated extracts in the TTR-binding assay; 4) to perform targeted chemical analyses of PFAS in sediment; 5) to compare TTR binding of the sediment extract with expected TTR binding based on concentrations measured using targeted chemical analyses and TTR-binding potencies measured for the individual PFAS; and 6) to perform suspect screening on extract fractions showing TTR binding that could not be assigned to the PFAS quantified using targeted chemical analyses.

METHODS

Standards of 31 individual PFAS, solvent blank, solvent spiked with PFAS standards, extract of unspiked sediments, extracts of sediments spiked with PFAS standards, extract of the polluted environmental sediment (unfractionated), and fractionated extract of the polluted environmental sediment were tested in the TTR-binding assay using microtiter plates and a liquid handling robot (epMotion 5075; Eppendorf). Targeted chemical analyses of 52 PFAS were performed on the environmental sediment extract (full names and abbreviations are in the Supporting Information, Table S2). The difference in the number of standards tested in the TTR-binding assay and the number used for targeted chemical analyses was due to standard availability and the cost of acquiring sufficient standard materials for testing in the assay. Suspect screening was performed in the retention time window corresponding to extract fractions that showed TTR-binding activity that could not be explained by the results of the targeted analyses. Further details are provided in the following sections.

TTR-binding assay

The TTR-binding assay was developed to evaluate whether substances can compete with T_4 for binding to TTR (Ren & Guo, 2012). The TTR-binding assay is a competitive binding assay using a fluorescent conjugate of T_4 and fluorescein 5-isothiocyanate (FITC). The principle of the TTR-binding assay is that the FITC-T_4 conjugate has a higher fluorescence intensity when its T_4 group is bound to TTR than when its T_4 group is unbound, due to intramolecular quenching of the FITC group by the free T_4 group. Thus, competitive binding of other substances to TTR results in displacement of bound FITC-T_4 from the TTR and consequently more free FITC-T_4 in the assay, which can be quantified as a decrease in fluorescence. The method, which was originally developed by Ren & Guo (2012), was performed as described by Jonkers et al. (2022), with one modification, that is, incubations were performed in the dark for 5 min on a plate shaker (600 rpm, Titramax 1000; Heidolph), followed by a 15-min incubation without shaking. The final volume of the assay was 200 µl.

Standards of individual PFAS

Standards of 31 individual PFAS were purchased from multiple suppliers, as indicated in Table 1. For each standard, concentration series were prepared. Methanol was used as the

TABLE 1: Details for thyroxine and standards of 31 individual per- and polyfluorinated substances tested in the transthyretin-binding assay ($n = 2$)

Group	Name	CAS no.	Abbreviation	Structure	No.	Supplier	IC50 (μM)	SD (μM)	REP
	Thyroxine		T_4				0.074	0.032	1
PFSA	Perfluorobutane sulfonic acid	375-73-5	PFBS	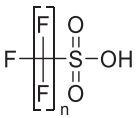	4	Sigma-Aldrich	12	2.6	0.0060
	Perfluorohexane sulfonic acid	3871-99-6	PFHxS		6	Fluka	0.56	0.14	0.13
	Perfluoroheptane sulfonic acid	375-92-8	PFHpS		7	Toronto Research Chemicals	0.31	0.31	0.24
	Perfluorooctane sulfonic acid	2795-39-3	PFOS		8	Fluka	0.29	0.052	0.26
	Perfluorodecane sulfonic acid	335-77-3	PFDS		10	Toronto Research Chemicals	35	24	0.0021
PFOS precursors	Perfluorooctane sulfonamide	754-91-6	FOSA			ABCR	0.59	0.092	0.13
	N-ethyl perfluorooctane sulfonamido ethanol	1691-99-2	EtFOSE	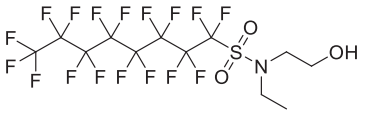		Toronto Research Chemicals	4.3	1.9	0.017
	N-ethyl perfluorooctane sulfonamidoacetic acid	2991-50-6	EtFOSAA	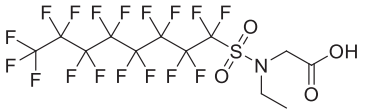		Toronto Research Chemicals	8.5	1.7	0.0086
Other PFSA precursors	Perfluoro-1-butane sulphonamide	30334-69-1	FBSA	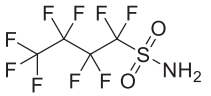		ABCR	44	7.3	0.0017
	Perfluoro-1-hexane sulfonamide	41997-13-1	FHxSA	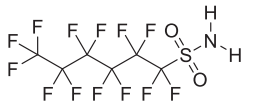		ABCR	1.1	0.41	0.065
	N-(3-(dimethyl-aminopropan-1-yl)-perfluoro-1-hexanesulfonamide	50598-28-2	N-AP-FHxSA	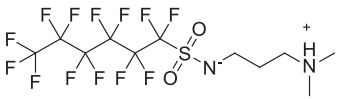		Key Organics	4.3	0.88	0.0017
PFCA	Perfluorobutanoic acid	375-22-4	PFBA		4	ABCR	—		
	Perfluoropentanoic acid	2706-90-3	PFPeA		5	Sigma-Aldrich	32	8.3	0.0023
	Perfluorohexanoic acid	307-24-4	PFHxA		6	Sigma-Aldrich	4.9	0.69	0.015
	Perfluoroheptanoic acid	375-85-9	PFHpA		7	Acros	0.48	0.092	0.15
	Perfluorooctanoic acid	335-67-1	PFOA		8	Fluka	0.40	0.071	0.18
	Perfluorononanoic acid	375-95-1	PFNA	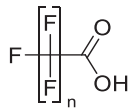	9	Sigma-Aldrich	0.81	0.20	0.091
	Perfluorodecanoic acid	335-76-2	PFDA		10	Sigma Aldrich	1.8	0.25	0.042
	Perfloroundecanoic acid	2058-94-8	PFUnDA		11	Sigma-Aldrich	0.95	0.10	0.077
	Perfluorododecanoic acid	307-55-1	PFDoDA		12	Sigma-Aldrich	1.8	0.49	0.041
	Perfluorotridecanoic acid	72629-94-8	PFTrDA		13	Sigma-Aldrich	3.3	2.3	0.022

(*Continued*)

TABLE 1: (*Continued*)

Group	Name	CAS no.	Abbreviation	Structure	No.	Supplier	IC50 (μM)	SD (μM)	REP
	Perfluorotetradecanoic acid	376-06-7	PFTeDA		14	Sigma-Aldrich	3.3	5.8	0.022
	Perfluoroexadecenoic acid	67905-19-5	PFHxDA		16	Toronto Research Chemicals	5.8	0.7	0.013
Fluoro-telomers	5:3 Fluorotelomer carboxylic acid	914637-49-3	5:3 FTCA	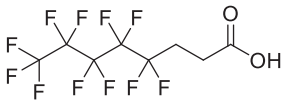		Toronto Research Chemicals	5.9	1.1	0.012
	6:2 Fluorotelomer sulfonic acid	27619-97-2	6:2 FTS	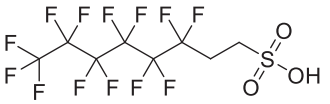		ABCR	12	3.0	0.0063
	6:2 Fluorotelomer alcohol	647-42-7	6:2 FTOH	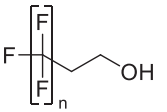	6	ABCR	—		
	8:2 Fluorotelomer alcohol	678-39-7	8:2 FTOH		8	ABCR	—		
Fluoro-ethers	Hexafluoropropylene oxide dimer acid	13252-13-6	HFPO-DA	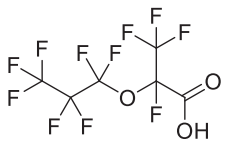		ABCR	25	4.3	0.0030
	Hexafluoropropylene oxide trimer acid	13252-14-7	HFPO-TA	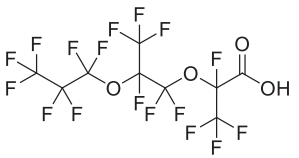		ABCR	1.6	0.39	0.047
Fluoro-acrylates	Tridecafluorooctyl acrylate	17527-29-6	TFOA	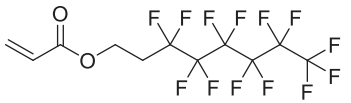		ABCR	0.61	0.29	0.12
	Heptadecafluorodecyl acrylate	27905-45-9	HDFDA	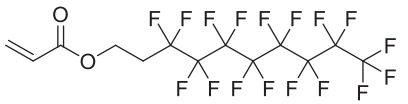		ABCR	—		

The table shows the per- and polyfluorinated substance (PFAS) group, full name of substances, CAS number, abbreviation, structure, number of repeating units (No.), supplier, average half-maximal inhibitory concentrations (IC50), standard deviation (SD), and relative potency (REP).
PFCA = polyfluoroalkyl carboxylic acid; PFSA = perfluorosulfonic acid.

carrier solvent instead of the dimethyl sulfoxide (DMSO) that is usually used in the TTR-binding assay. The reason for this was because hexafluoropropylene oxide dimer acid (HFPO-DA) has been reported to be unstable in DMSO, as well as in acetone and acetonitrile, whereas it is stable in methanol (Liberatore et al., 2020; Zhang et al., 2021).

Sediment extracts

Sediment sampling. A sediment sample was collected in the Randselva River (Norway) downstream of a shut-down factory that had produced PFAS-coated paper products. The factory and the river are located upstream from Lake Tyrifjorden (Norway). River and lake sediments downstream of the factory have previously been reported to be heavily polluted with PFAS, including a range of large, hydrophobic, precursor PFAS (i.e., precursors to perfluoroalkyl carboxylic acids [PFCA] and perfluoroalkyl sulfonic acids [PFSA]), in addition to significant amounts of unknown fluorinated organic substances (Langberg et al., 2020, 2021). Finally, sediments that were considered as representative of environmental concentrations in areas not directly affected by point sources were sampled upstream from the factory to be used for spike experiments (referred to as upstream sediments hereafter).

Spike experiments. To verify the efficiency of the TTR-binding assay on fractionated sample extracts, solvent and upstream sediments (sampled upstream of the factory; see the *Sediment sampling* section) were spiked with 35 pmol (low spiked) or 310 pmol (high spiked) of each individual standard of perfluorohexane sulfonic acid (PFHxS), perfluorooctanoic acid (PFOA), perfluorooctane sulfonic acid (PFOS), and perfluorooctane sulfonamide (FOSA). Based on the assumption that 100% of each individual PFAS ended up in one single sample fraction, and taking account of the final test volume of the TTR-binding assay being 200 µl, these spike levels correspond to a final concentration in the assay after fractionation of 175 nM for the low spiked sediments and 1550 nM for the high spiked sediments.

Quality control. A blank sample using clean solvent and a sample of unspiked upstream sediments (sampled upstream of the factory; see the *Sediment sampling* section) were tested in the TTR-binding assay (see Figure 1 and Supporting Information, S1). In addition, procedure blanks were tested before and after the spike experiments to check for cross-contamination.

Extraction. Ten grams of wet sediment was extracted using acetonitrile and ultrasonication. Extracts were divided into two aliquots, one for chemical analyses (for which mass-labeled analytical standards were then added) and one for testing in the TTR-binding assay (without adding mass-labeled analytical standards). Cleanup of extract to be tested in the TTR-binding assay was performed using active carbon (ENVICarb; Sigma-Aldrich). Recovery tests were performed to ensure that the cleanup method did not remove significant amounts of PFAS

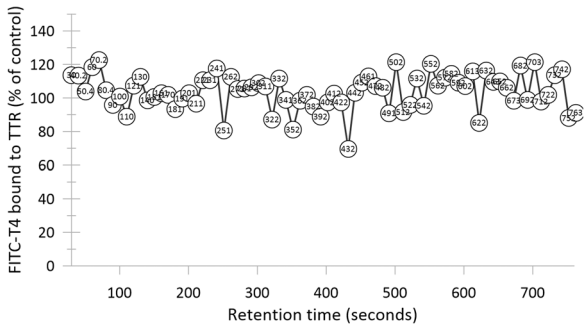

FIGURE 1: Unspiked sediments. Observed fluorescein isothiocyanate (FITC)-thyroxin (T_4) fluorescence (% of control) as an indicator of transthyretin (TTR) inhibition on extract of unspiked sediment. Numbers within the white circles refer to the retention time (s) at the start of each fraction.

(Supporting Information, Table S1). Detailed extraction protocols are given in the Supporting Information.

Fractionation of sample extracts. Procedure blanks, spiked solvent, extracts of spiked upstream sediment, and extract of the environmental sediment sample were fractionated using a chromatography method modified from Guelfo & Higgins (2013) and the FractioMate™ fraction collector (Spark Holland; Jonker et al., 2019). Extracts were separated into 10-s fractions on a 96-well plate. The exact starting time for the different fractions varied (on average <0.5 s) between each run. To account for this minimum variation, fractions were named after the exact starting times logged by the FractioMate. Detailed descriptions of extract treatment and volumes used for fractionation are given in the Supporting Information.

Chemical analyses

Target analyses. Target quantitative analysis was performed for 52 PFAS. The PFAS were confirmed using a signal:noise ratio of 10:1, a mass error <10 ppm, and a retention <0.5 compared with the analytical standard. All labeled and native analytical standards were purchased from Wellington Laboratories. A calibration curve (0.2–1000 pg, $R^2 > 0.99$) was applied to each target PFAS. Branched and linear isomers, when present, were reported together. Continuing calibration verification (CCV) and instrument blanks were run every 10 samples to confirm instrument performance. The CCVs were 70% to 130% for each target PFAS. Reporting limits were calculated for each analyte based on the lower point of the calibration curve that met the criteria and was within 30% of the known value or three times the highest blank concentration, whichever was higher. The PFAS identified in the environmental sediments using target analyses are shown in Tables 2 and 3. Details are provided in the Supporting Information.

Suspect screening. Suspect screening was performed using a custom-extracted ion chromatogram list containing PFAS from the literature and their theoretical homologs (Nickerson et al., 2021). An inhouse tandem mass spectrometry spectral library containing more than 300 PFAS spectra was used to

TABLE 2: Details for individual per- and polyfluorinated substances identified in environmental sediment but not tested in the transthyretin-binding assay

Group	Name	Abbreviation	Structure	No.	Identification method
PFSA	Perfluoropropane sulfonic acid	PFPrS	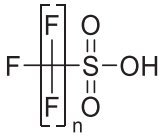	3	TA
	Perfluoropentane sulfonic acid	PFPeS		5	TA
	Perfluorononane sulfonic acid	PFNS		9	TA
	Perfluorododecane sulfonic acid	PFDoDS		12	TA
PFOS precursors	Perfluorooctane sulfonamidoacetic acid	FOSAA	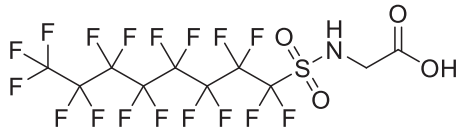		TA
	N-methyl perfluorooctane sulfonamidoacetic acid	MeFOSAA	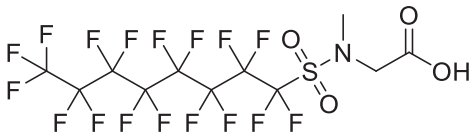		TA
	N-methyl perfluorooctane sulfonamide	MeFOSA	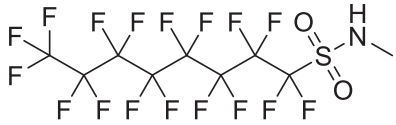		TA
	N-ethyl perfluoroctane sulfonamide	EtFOSA	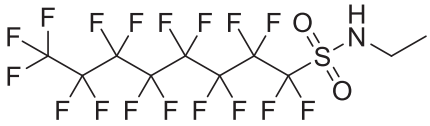		TA
PFCA	Perfluorooctadecanoic acid	PFODA	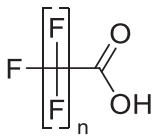	18	TA
Fluorotelomers	4:2 Fluorotelomer sulfonic acid	4:2 FTS	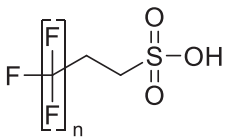	4	TA
	8:2 Fluorotelomer sulfonic acid	8:2 FTS		8	TA
	10:2 Fluorotelomer sulfonic acid	10:2 FTS		10	TA
	12:2 Fluorotelomer sulfonic acid	12:2 FTS		12	SS
	14:2 Fluorotelomer sulfonic acid	14:2 FTS		14	SS
	6:2 Unsaturated fluorotelomer carboxylic acid	6:2 UFTCA	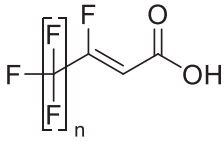	5	TA
	8:2 Unsaturated fluorotelomer carboxylic acid	8:2 UFTCA		7	TA
	10:2 Unsaturated fluorotelomer carboxylic acid	10:2 UFTCA		9	TA
	6:2 Saturated fluorotelomer carboxylic acid	6:2 FTCA	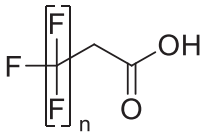	6	TA
	8:2 Saturated fluorotelomer carboxylic acid	8:2 FTCA		8	TA
	10:2 Saturated fluorotelomer carboxylic acid	10:2 FTCA		10	TA
	10:3 Saturated fluorotelomer carboxylic acid	10:3 FTCA	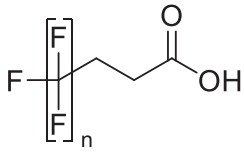	10	SS

(*Continued*)

TABLE 2: (*Continued*)

Group	Name	Abbreviation	Structure	No.	Identification method
diPAP	6:2 Polyfluoroalkyl diesterphosphate	6:2 diPAP	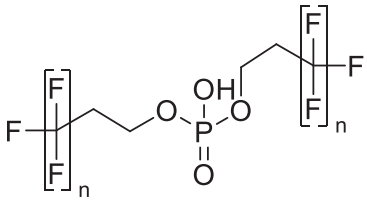	6	TA
	6:2/8:2 Polyfluoroalkyl diesterphosphate	6:2/8:2 diPAP		6/8	TA
	8:2 Polyfluoroalkyl diesterphosphate	8:2 diPAP		8	TA
	10:2 Polyfluoroalkyl diesterphosphate	10:2 diPAP		10	SS
SAmPAP	Di-substituted phosphate ester of N-ethyl per- fluorooctane sulfonamido ethanol	SAmPAP diester	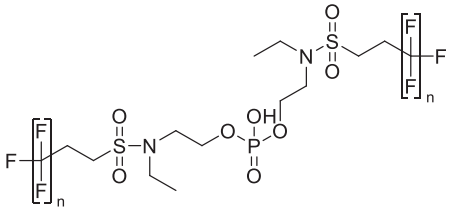	8	TA
Perfluoro-4-ethylcyclohexane sulfonate		PFEtCHxS	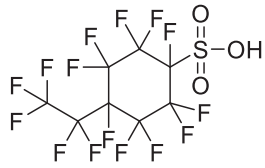		TA
10:2 1,2-di(hydroxymethyl) fluorotelomer thia propanoic acid		10:2 di(MeOH)-FTTh-PrA	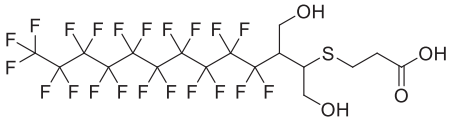		SS

The table shows per- and polyfluorinated substances group, full name of substances, abbreviation, structure, number of repeating unit (No.), and identification method. PFSA = polyfluorosulfonic acid; PFCA = polyfluoroalkyl carboxylic acid; TA = target analyses; SS = suspect screening.

confirm features when available. If a peak had a low area count ($<10^6$) and no supporting information like a matching spectra or part of a homolog series, then it was removed from the suspect list. Suspect compounds that were not excluded were semi-quantitated following the approach described by Nickerson et al. (2020). The PFAS identified in the environmental sediments using suspect screening are shown in Table 2. Details of the suspect screening are provided in the Supporting Information.

Aligning retention times. Sample fractionation and testing in the TTR-binding assay were performed at the Vrije Universiteit Amsterdam (VUA; The Netherlands), and chemical analyses were performed at the Colorado School of Mines (Mines; Golden, CO, USA) using the same LC setup. Retention times were aligned between both laboratories by a linear regression on the retention times determined for a range of PFAS standards in both laboratories (Supporting Information, Table S3 and Figure S2). Using this regression, bioactive fractions determined at VUA were linked—based on their retention time—to features determined at corresponding retention times at Mines.

Calculating the T_4-equivalent concentration

To make meaningful comparisons between concentrations of individual substances in the assay, each concentration of an individual $PFAS_i$ that was tested in the assay was calculated into a corresponding T_4 equivalent concentration ($T4EQ_i$) by multiplying it by its relative TTR-binding potency compared with T_4 using Equation (1).

$$T4EQ_i = REP_i \times C_i = \frac{IC50_{T4}}{IC50_i} \times C_i \quad (1)$$

where $T4EQ_i$ is the concentration of $PFAS_i$ expressed as a concentration of T_4 (nM) with similar TTR-binding potency, REP_i is the relative potency of $PFAS_i$ to bind TTR compared with T_4, which is calculated by dividing the median inhibitory concentration for T_4 ($IC50_{T4}$ in nM) by the median inhibitory concentratios for each individual $PFAS_i$ ($IC50_i$ in nM), and C_i is the concentration of the individual $PFAS_i$ in the assay (nM). The total TTR-binding potency of the identified PFAS/fraction was calculated as a T4EQ concentration by summarizing all $T4EQ_i$ concentrations of the individual PFAS present in that fraction.

RESULTS AND DISCUSSION

TTR binding by individual PFAS standards

In the TTR-binding assay, an IC50 of 74 nM was determined for T_4. For the tested standards of PFAS, IC50 values varied depending on the number of perfluorinated and hydrogenated

TABLE 3: Dry weight sediment concentrations, retention times (chromatogram peak), and concentrations in the bioassay, for targeted per- and polyfluorinated substances

PFAS	Conc. in sediment (μg kg^{-1} dry wt)	Retention time (s)	Conc. in bioassay (nM)	T4EQ (nM)	Fraction	Sum T4EQ/ fraction (nM)	Expected FITC-T_4 remaining bound to TTR/fraction (% of control)
PFBA	5	174	135	0	170	0	
PFPrS	0.02	192	1		191		
PFPeA	9	222	169	0.4	220	0.4	99
PFBS	0.5	228	8	0.05	230	0.05	100
4:2 FTS	1	264	9		261		
PFHxA	26	270	436	7	261	7	89
PFPeS	0.1	276	1		271		
PFHxS	2	318	25	3	311		
PFHpA	41	318	597	93	311	96	55
6:2 UFTCA	0.9	329	14		321		
6:2 FTCA	1.9	331	26		331		
PFEtCHxS	2	354	27		351		
6:2 FTS	34	354	418	3	351		
FHxSA	0.1	355	1	0.04	351		
PFOA	315	360	3993	739	351		
PFHpS	10	360	119	28	351	770	29
PFOS	1980	396	20 750	5313	391		
PFNA	52	396	583	53	391	5366	20
8:2 UFTCA	5	407	58		401		
8:2 FTCA	12	410	133		401		
FOSAA	38	426	359		422		
PFDA	294	426	3002	125	422		
8:2 FTS	1033	426	10 255		422		
PFNS	1	427	8		422	125	50
FOSA	64	432	671	84	431	84	57
MeFOSAA	1868	444	17 137		442		
PFDS	2	456	18	0.04	452		
PFUnDA	81	456	753	58	452		
EtFOSAA	11 957	456	107 063	928	452	986	27
MeFOSA	1	468	7		461		
10:2 UFTCA	3	470	25		461		
10:2 FTCA	28	472	251		472		
PFDoDA	272	480	2317	96	472		
10:2 FTS	487	480	4058		472	96	55
EtFOSA	17	483	166		482		
6:2 diPAP	1	486	5		482		
PFTrDA	80	504	634	14	502		
PFDoDS	1	504	5		502	14	82
PFTeDA	208	522	1527	34	521	34	71
6:2/8:2 diPAP	3	542	16		542		
PFHxDA	19	558	122	2	552	2	96
8:2 diPAP	4	566	20		562		
PFODA	5	588	27		582		
SAmPAP diester	75 589	599	328 566		592		

T4EQ concentrations in the extract are listed for the PFAS for which standards were tested in the TTR-binding assay (listed in Table 1). Summed T4EQ values and expected percentage of T_4 bound to TTR are shown for the fractions containing PFAS tested in the TTR-binding assay.
FITC = fluorescein 5-isothiocyanate; PFAS = per- and polyfluoroalkyl substances; T4EQ = thyroxin equivalent; T_4 = thyroxin; TTR = transthyretin; FHxSA = perfluorohexane sulfonamide. For other abbreviations, see Table 1 or Table 2.

carbon atoms, the functional group, and, for PFSA precursors, the size or number of atoms in the group(s) attached to the nitrogen in the precursors (Table 1). Concentration–response curves for the tested PFAS standards are shown in the Supporting Information, Figure S3.

The most potent PFAS were the eight- and seven-carbon PFSA (PFOS and perfluoroheptane sulfonic acid [PFHpS]) and the eight-carbon PFCA (PFOA), which showed approximately 4 to 5-times weaker potencies, compared with T_4. Shorter PFSA and PFCA showed decreasing potencies with decreasing number of carbons, whereas longer PFSA and PFCA showed decreasing potencies with increasing number of carbons. Of the precursors to PFOS, FOSA was the most potent, (approximately 8 times weaker compared with T_4). The two other tested PFOS precursors, N-ethyl-perfluorooctane sulfonamide (EtFOSE) and N-ethyl-perfluorooctane sulfonamidoacetic acid (EtFOSAA), showed much weaker potencies. Considering all PFOS precursors together, TTR-binding potencies seemed to decrease with increasing size and/or number of atoms in the group(s) attached to the nitrogen (see structures in Table 1).

A similar trend was shown for the PFHxS precursors (based on their structures), whereby the six-carbon FOSA homolog,

perfluorohexane sulfonamide (FHxSA) was more potent compared with the larger N-(3-dimethylaminopropan-1-yl)perfluoro-1-hexane-sulfonamide (N-AP-FHxSA). Furthermore, perfluoro-1-butane sulphonamide (FBSA), FHxSA, and FOSA are homologs with varying numbers of perfluorinated carbons (4, 6, and 8, respectively). As for PFSA and PFCA, the potencies of these precursors varied with chain length and the most potent substance was again the eight-carbon homolog. For the fluorotelomers, it was not possible to interpret trends based on our results. However, it is clear that potencies varied depending on functional group because clear binding was observed for 6:2 fluorotelemer sulfonate (6:2 FTS) and 5:3 fluorotelemer carboxylic acid (5:3 FTCA), whereas no binding was observed for the 6:2 fluorotelemer alcohol (6:2 FTOH) or 8:2 FTOH. For the tested fluorinated ethers, the highest TTR-binding potency was observed for the largest of the two, HFPO-TA. For the fluoroacrylates, tridecafluorooctyl acrylate (TFOA) showed a relatively strong potency, whereas no TTR binding was observed for the longer chained heptadecafluorodecyl acrylate (HDFDA).

The potencies we report for the individual PFAS are in overall agreement with previously reported trends for IC50 values for polyfluorbutanoic acid (PFBA), perfluorohexanoic acid (PFHxA), perfluoroheptanoic acid (PFHpA), PFOA, perfluorononanoic acid (PFNA), perfluorodecanoic acid (PFDA), perfluoroundecanoic acid (PFUnDA), perfluorododecanoic acid (PFDoDA), perfluorotetradecanoic acid (PFTeDA), perfluorobutane sulfonic acid (PFBS), PFHxS, PFOS, and FOSA (Hamers et al., 2020; Weiss et al., 2009). The study by Weiss et al. (2009) used a radioligand binding assay. In line with the present study, Weiss et al. (2009) reported that 6:2 FTOH and 8:2 FTOH had no potencies in the assay. In addition, a relatively strong potency was reported for FOSA, whereas no TTR binding was observed for EtFOSE (Weiss et al., 2009), similar to the relatively large differences in potencies between the two in the present study. Thus, the results for the individual substances were reproduceable and considered to be reliable estimates of TTR inhibition.

Several of the PFAS that had not been tested in the TTR-binding assay before had weak or no binding potencies. For example, several of the tested fluorotelomers, fluoroethers, and fluoroacrylates, had IC50 values >10 000 nM or did not exhibit any TTR-binding potency within the concentration range tested (Supporting Information, Figure S3). The same applied for the PFCA shorter than PFHxA. Thus the TTR-binding assay cannot be considered as a PFAS-specific bioassay. In addition, compounds other than PFAS, including many halogenated phenols, are known to be strong TTR-binding compounds (see Weiss et al., 2015 for an extensive overview). Therefore, an observed response could be caused by compounds other than PFAS, which further complicates the use of the TTR-binding assay as a PFAS-specific assay.

Sediment extracts. Fluorescence in the different fractions of the quality control samples tested in the TTR-binding assay varied between 70% and 130% for the extract of unspiked upstream sediment (Figure 1) and clean solvent (Supporting Information, Figure S1). Thus, this variation was considered the methodological noise.

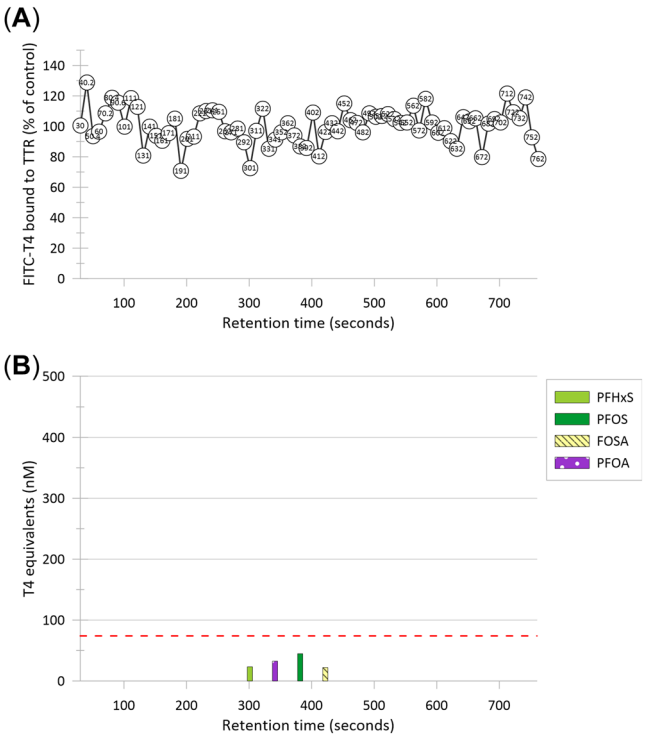

FIGURE 2: Spiked sediments: Observed fluorescein isothiocyanate (FITC)-thyroxin (T_4) fluorescence (% of control) as an indicator of transthyretin (TTR) inhibition (**A**) and calculated T_4-equivalent (T4EQ) concentrations in nM (**B**) for perfluorohexane sulfonic acid (PFHxS), perfluorooctanoic acid (PFOA), perfluorooctane sulfonic acid (PFOS), and perfluorooctane sulfonamide (FOSA) in the different fractions in the low (175-nM) spiked sediments. The dashed red line indicates the median inhibitory concentration (IC50) for T_4 at 74 nM. Numbers within the white circles refer to the retention time (s) at the start of each fraction.

Spike experiments. Similar results were obtained for the spiked solvent and sediments. No fluorescence below 70%, and therefore no clear inhibition, was observed for the unspiked and low-spiked solvent and sediments, respectively (Figures 1 and 2 and Supporting Information, Figures S1 and S4). However, for the high-spiked solvent and sediments, inhibition was observed (Figure 3 and Supporting Information, Figure S5). For the high-spiked sediment, inhibition was observed for fractions starting with retention times 301, 341, and 372 s (Figure 3). These fractions corresponded to measured retention times for PFHxS, PFOA, and PFOS, respectively. In contrast, no clear inhibition was observed for fractions with retention times corresponding to the retention time for FOSA (409–438 s) in either the spiked sediments or the spiked solvent.

Based on the assumption that 100% of each individual PFAS ended up in one, single sample fraction, and taking account of the final test volume of the TTR-binding assay being 200 µl, the TTR-binding potencies were calculated according to Equation (1). The concentrations of the four PFAS in the low-spiked sediment were calculated as TTR-binding potencies corresponding to 22 to 45 nM T4EQ concentrations, which is lower than the IC50 value for T_4 (74 nM; Figure 2). Considering that the chromatogram peaks had a 30-s peak width in retention

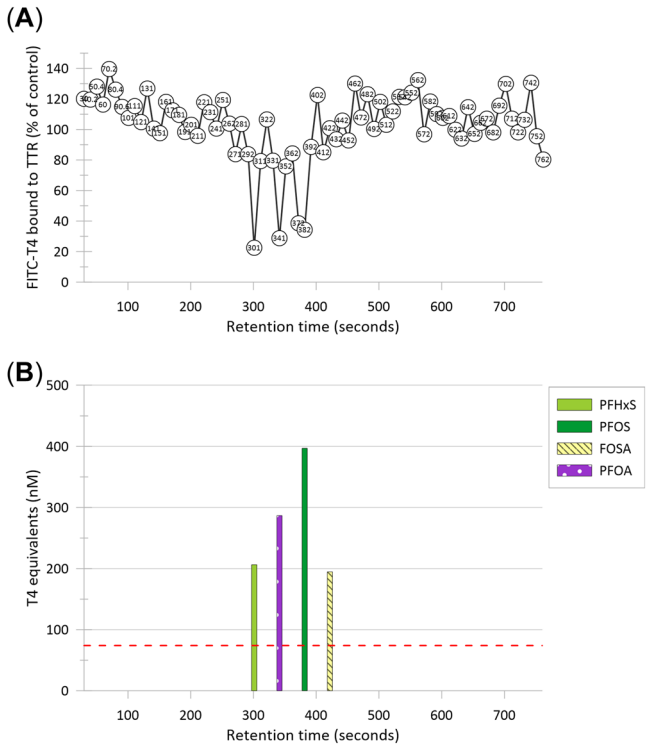

FIGURE 3: Spiked sediments. Observed fluorescein isothiocyanate (FITC)-thyroxin (T_4) fluorescence (% of control) as an indicator of transthyretin (TTR) inhibition (**A**) and calculated T_4-equivalent concentrations in nM (**B**) for perfluorohexane sulfonic acid (PFHxS), perfluorooctanoic acid (PFOA), perfluorooctane sulfonic acid (PFOS), and perfluorooctane sulfonamide (FOSA) in the different fractions in the high (1550-nM) spiked sediments. The dashed red line indicates the median inhibitory concentration (IC50) for T_4 at 74 nM. Numbers within the white circles refer to the retention time (s) at the start of each fraction.

times, it is unlikely that all of an individual PFAS ended up in only one 10-s fraction, possibly explaining the lack of an observed response. In contrast, the concentrations of the four PFAS in the high-spiked sediment had TTR-binding potencies corresponding to 195 to 397 nM T4EQ concentrations, which were all more than 2.5 times higher than the IC50 value for T_4 (Figure 3). Thus, clear inhibition was expected for the fractions with the majority of a PFAS even if the individual PFAS did not end up in a single fraction. The observed inhibition in both fractions 372 and 382 is likely due to PFOS eluting into both these fractions. The lack of a clear inhibition for the fractions with retention times corresponding to FOSA was unexpected. The FOSA standard showed a relatively high potency in the TTR-binding assay. It is possible that FOSA eluted into several fractions and thus that the concentrations in each fraction were too low to be detected. Nevertheless, the spike experiment showed that PFAS in sediments exhibit inhibition in specific fractions, and thus show that substances, with affinity for TTR, in sediments can be detected using the TTR-binding assay.

Environmental sediment. Unfractionated whole extract (2 µl; see the Supporting Information) of the sediment sample collected directly downstream of the factory showed TTR-binding equivalent to a T_4 concentration of 91 nM. Therefore, it was concluded that TTR-binding substances had been extracted from the sediment. The PFAS identified in the environmental sediments using target analyses are shown in Tables 2 and 3.

All fractions were named after their starting time in seconds. The fractionated extract of the sediment sample collected directly downstream of the factory showed fluorescence below 70% of the control in all fractions with retention times between 291 and 592 s (Figure 4A). The strongest inhibition was generally shown for fractions 311 to 482 s.

As for the spiking experiment, concentrations of all targeted PFAS above the quantification limit in the extract were calculated into bioassay concentrations based on the assumption that 100% of each individual PFAS ended up in one, single sample fraction, and taking account of the final test volume of the TTR-binding assay being 200 µl (Table 3). It has previously been reported that the TTR-binding potencies of mixtures are well predicted by concentration addition (Hamers et al., 2020). Thus, concentrations of targeted PFAS with available IC50 values (Table 1) were calculated into T4EQ concentrations (Equation 1), which were assigned to the fractions corresponding to their retention time. The T4EQ concentrations of PFAS ending up in the same fractions were summed. The expected percentage of T_4 bound to TTR was calculated for the fractions with a T4EQ using the equation for the T_4 concentration–response curve (Supporting Information, Figure S3A), shown in Table 3.

For seven fractions, relatively high T4EQ concentrations were calculated based on the concentrations and known TTR-binding potencies of the targeted PFAS (Figure 4B). All of these seven sample fractions were within the retention time span of fractions 311 to 472. These seven fractions were (named after their starting time in seconds): 311 (96 nM T4EQ), dominated by PFHpA and a small amount of PFHxS; 351 (770 nM T4EQ), dominated by PFOA and small amounts of 6:2 FTS and PFHpS; 391 (5313 nM T4EQ), with PFOS and some PFNA; 422 (125 nM T4EQ), containing PFDA; 431 (84 nM T4EQ) containing FOSA; 452 (986 nM T4EQ), containing EtFOSAA and PFUnDA; and 472 (96 nM T4EQ) with only PFDoDA (Figure 4B). Unlike the spike experiments (Figure 3 and Supporting Information, Figure S5), the fraction where FOSA was expected to elute (fraction 431) showed clear inhibition. The reason for the discrepancy is not clear. Nevertheless, as indicated in Table 3, the T4EQ for these seven fractions explained much of the observed inhibition. (The expected FITC-T_4 remaining bound to TTR was 55% of control for fraction 311, 29% for fraction 351, 20% for fraction 391, 50% for fraction 422, 57% for fraction 431, 27% for fraction 452, and 55% for fraction 472.) Thus, much of the inhibition observed for these seven fractions can be explained by the capacity of the targeted PFAS to bind to TTR.

In addition to the seven sample fractions just discussed, there was also reported inhibition for the other fractions corresponding to retention times between 311 and 482 s. For example, the sample fraction with the second strongest TTR binding (381) was not among these seven. A similar result was observed for the high-spiked sediments and is likely due to PFOS eluting into both fractions 381 and 391. Greater peak spreading (i.e., longer chromatographic peaks resulting in

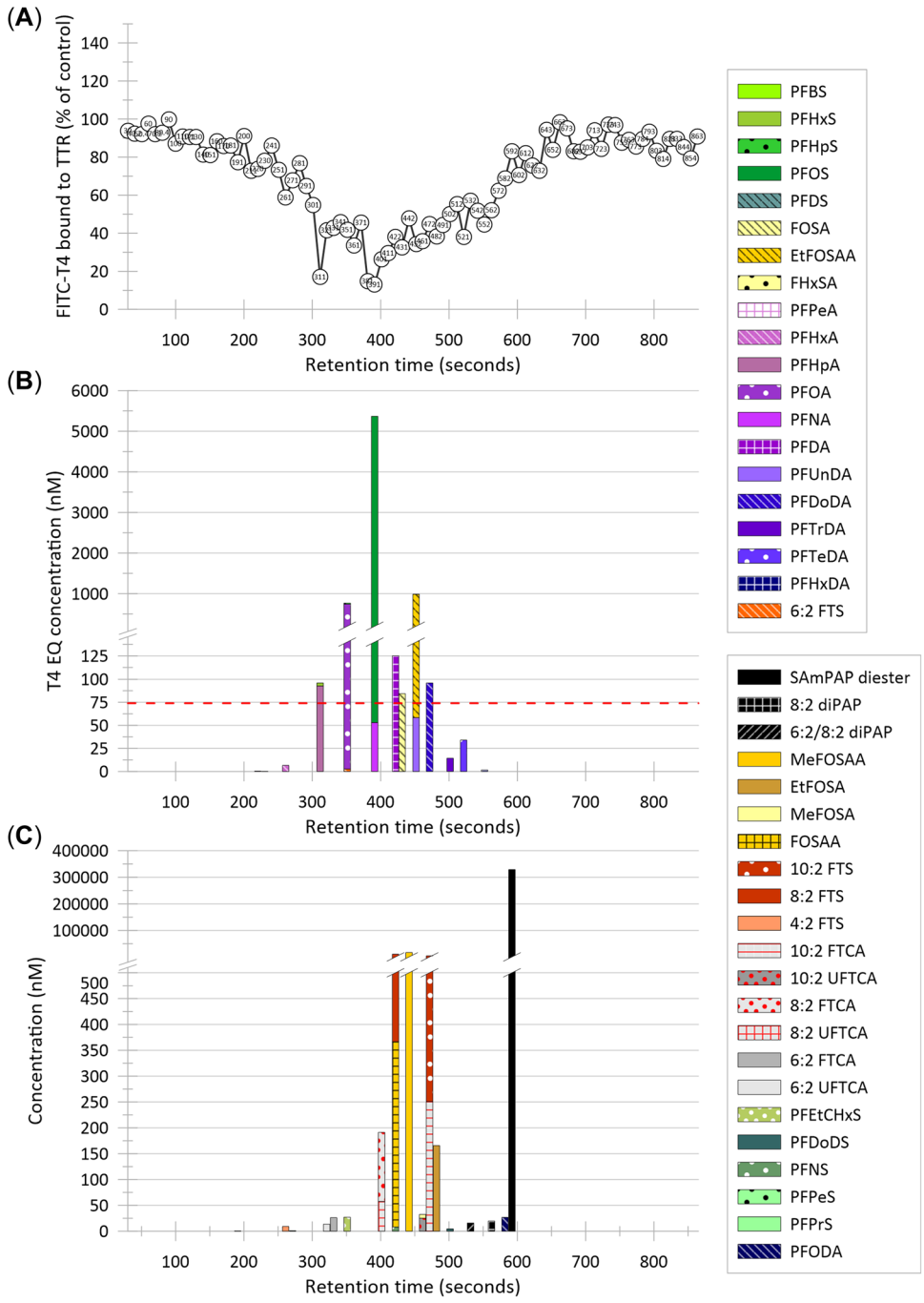

FIGURE 4: Fractionated extract of environmental sediment. The *x*-axis refers to the retention time (s) at the start of each fraction. (**A**) Bioassay response. Numbers within the white circles refer to the retention time (s) at the start of each fraction. (**B**) Calculated thyroxin (T_4)-equivalent (T4EQ) concentrations (nM, bars) for the targeted per- and polyfluorinated substances (PFAS). The dashed red line indicates the T_4 median inhibitory concentration (IC50) at 74 nM. (**C**) Concentrations of targeted PFAS without an established IC50 value. Note that there is a break and a change in scale in the *y*-axis for **B** and **C**. FHxSA, perfluorohexane sulfonamide; PFDoDS, perfluorododecane sulfonic acid. For other abbreviations, see Table 1 or Table 2.

substances being collected in multiple sample fractions) likely explains at least some of the discrepancy. However, the results might also indicate that other substances with potency for TTR binding were present in the sample extract.

Unfortunately, T4EQ concentrations could not be calculated for all targeted substances, because they have not all been tested for their TTR-binding potencies. Bioassay concentrations for these targeted substances without an established IC50 value are shown in Figure 4C. Of these, the highest concentration was reported for perfluorooctance sulfonamide phosphate (SAmPAP) diester (329 µM, RT: 599 s) followed by N-methyl perfluorooctane sulfonamidoacetic acid (MeFOSAA; 17 µM, RT: 444 s), 8:2 FTS (10 µM, RT: 426 s), and 10:2 FTS (4 µM, RT: 480 s). Lower concentrations were observed for

FOSAA (359 nM, RT: 426 s), 10:2 fluorotelomer carboxylic acid (10:2 FTCA; 251 nM, RT: 472 s), EtFOSA (165 nM, RT: 483 s), and 8:2 FTCA (133 nM, RT: 410 s; where RT is retention time).

The high concentrations of SAmPAP diester, other PFOS precursors (e.g., FOSA, EtFOSAA, FOSAA, and EtFOSA) and FTS in the sample extract is in agreement with previously reported concentrations in sediments downstream of the factory, reflecting the historic use of these compounds in the paper industry (Langberg et al., 2021). Fractions corresponding to the retention time for SAmPAP diester (599 s) did not show a clear inhibition (Figure 4), suggesting that SAmPAP diester has a very low potency for TTR binding, if any. The N-alkyl–substituted PFOS precursors reported in Table 1 showed a trend of decreasing TTR-binding potency with increasing size: the low potency of SAmPAP diester is in line with this observation. The high concentration of MeFOSAA, based on the retention time, is expected to have eluted into fraction 442, which is the sample fraction between the fractions where FOSA (431) and EtFOSAA (452) eluted. Based on the assumption that the N-alkylated PFOS precursors exhibit decreasing potencies with increasing size, MeFOSAA is expected to have a potency comparable to that of EtFOSE or EtFOSAA (IC50 values of 4253 and 8539 nM, respectively). Thus, the concentration of MeFOSAA (17,137 nM) likely contributes to the inhibition observed for the 442 fraction, and potentially also nearby fractions. It was expected that FOSAA would elute in the 422 fraction, together with PFDA. Based on its structure, FOSAA is expected to have a somewhat stronger potency compared with EtFOSAA (IC50 = 8539 nM). Nevertheless, the FOSAA concentration of 359 nM is likely too low to contribute significantly to the TTR-binding potency of this fraction, and most of the observed capacity to compete with FITC-T_4 is likely due to PFDA.

Based on the results reported in Table 1, no trends could be discerned for the structure-dependent TTR-binding potencies of FTS and FTCA, because only one PFAS from each group was available for testing (6:2 FTS and 5:3 FTCA, respectively). Nevertheless, based on the IC50 values for 6:2 FTS (11770 nM) and 5:3 FTCA (5918 nM), some of the observed inhibition in fractions with retention times of approximately 430 to 486 s is expected to be due to 8:2 FTS, 10:2 FTS, 8:2 FTCA, and 10:2 FTCA. For example, 10:2 FTS was expected to elute at the end of fraction 472 likely into the next fraction (482). For PFDoDA, which has the same retention time as 10:2 FTS, a T4EQ concentration of 96 nM was calculated (Table 3). In addition, EtFOSA mostly eluted into the 482 fraction. Therefore, compared with the 472 fraction, the stronger inhibition observed for the 482 fraction is likely due to EtFOSA combined with PFDoDA and 10:2 FTS ending up in the latter fraction. Thus, the reported inhibition observed for fractions 311 to 482 s can be mostly explained by the results of the targeted analyses of PFAS. However, the reported inhibition for fractions corresponding to retention times between 491 and 592 s was not fully explained by the targeted analyses.

To help evaluate the possibility that nontarget PFAS were present and contributing to TTR inhibition, suspect screening was performed to evaluate whether some of the observed inhibition in fractions 491 to 592 corresponded to the presence of nontargeted PFAS. Due to the width of the chromatographic peaks (as just discussed), suspect screening was also performed for fractions near the 491 to 592 fractions. Five candidate PFAS were identified (Table 2 and Supporting Information, Table S4): 10:2 1,2-di(hydroxymethyl) fluorotelomer thia propanoic acid (10:2 di(MeOH)-FTTh-PrA) and 10:3 FTCA (both with RT = 486 s, and sediment concentrations of 8 and 127 μg kg^{-1} dry wt, respectively), 12:2 FTS (RT = 526 s, sediment concentration of 3031 μg kg^{-1} dry wt, 14:2 FTS (RT = 567 s, sediment concentration of 1055 μg kg^{-1} dry wt), and 10:2 polyfluoroalkyl phosphoric acid diester [10:2 diPAP]; RT = 602 s, sediment concentration of 198 μg kg^{-1} dry wt). Unfortunately, no standards were available for these substances to confirm their chemical identity and their TTR-binding potency in the assay.

Based on their retention times in the nontarget analysis, 10:2 di(MeOH)-FTTh-PrA and 10:3 FTCA were expected to elute into the same 482 fraction as EtFOSA, and likely PFDoDA and 10:2 FTS (as just discussed). A relatively strong inhibition was observed for this fraction. It is thus likely that the observed inhibition for this fraction, as well as the somewhat weaker inhibition observed for nearby fractions, is in fact due to the combination of these five PFAS. However, based on the relatively low 10:2 di(MeOH)-FTTh-PrA concentration of approximately 8 μg kg^{-1}, this substance likely had a minor contribution to the observed potency. It was expected that 12:2 FTS would elute into the same 521 fraction as PFTeDA. A relatively strong TTR binding (replacing 62% of the FITC-T_4 bound to TTR) was observed for this fraction. The response was not fully explained by the concentration of PFTeDA, which corresponded to a T4EQ of 34—well below the IC50 value for T_4 (74 nM; see Table 3 and Figure 4). Therefore, the presence of 12:2 FTS could possibly explain some of the observed inhibition in fraction 521. The suspects 14:2 FTS and 10:2 diPAP were the only identified PFAS expected to elute into fractions 562 and 602, respectively. Therefore, because inhibition was observed for these fractions, 14:2 FTS and 10:2 diPAP are possible candidates. However, the inhibition was relatively weak for the 602 fraction, where 10:2 diPAP was expected to elute. Because this substance is relatively large and has a somewhat similar structure to SAmPAP diester, we speculate that this substance, like the SAmPAP diester, has a relatively low potency in the TTR-binding assay.

In addition to the suspect screening in fractions in and near the 491 to 592-s chromatographic windows, the substance perfluorooctane sulfinate (PFOSi, RT = 405 s) was screened for because it is a suspected transformation product on the transformation pathway from SAmPAP diester to PFOS (Benskin et al., 2013; Zhang et al., 2018), and it has been reported to be a relatively potent TTR-binding substance (approximately twice the IC50 value compared with PFOS; Weiss et al., 2009). A relatively low concentration of PFOSi was detected (approximate PFOSi sediment concentration of 10 μg kg^{-1} dry wt vs. 1980 μg kg^{-1} dry wt for PFOS). Therefore, the contribution of PFOSi to the observed TTR-binding potency of fraction 401 was likely minor.

The results we report show that much of the observed TTR-binding capacity of the extract of environmental sediment is

due to PFAS contamination. In addition, five novel candidate TTR-binding PFAS were identified in environmental sediment. Interestingly, the substance observed at the highest concentration, SAmPAP diester, probably did not contribute to the measured TTR-binding capacity. The SAmPAP diester has the potential for (bio)transformation into smaller PFAS (Zhang et al., 2018). Therefore, when it comes to TTR binding, the hazard associated with emissions of large amounts of this substance is mainly through (bio)transformation into more potent TTR-binding transformation products such as PFOS. The EDA approach we have demonstrated has proved valuable for prioritizing candidate PFAS not identified using conventional targeted chemical analyses, as possible endocrine-disrupting substances present in the environment.

Supporting Information—The Supporting Information is available on the Wiley Online Library at https://doi.org/10.1002/etc.5777.

Acknowledgments—Our research was funded by the Norwegian Research Council under the MILJØFORSK program (project number 268258/E50).

Conflict of Interest—Christopher P. Higgins is involved in various PFAS litigation activities. The other authors declare no conflicts of interest.

Author Contributions Statement—**Håkon A. Langberg**: Conceptualization; Formal analysis; Investigation; Writing—original draft. **Sarah Choyke**: Conceptualization; Formal analysis; Investigation; Writing—original draft. **Sarah E. Hale**: Conceptualization; Funding acquisition; Project administration; Supervision; Writing—review & editing. **Jacco Koekkoek**: Formal analysis; Investigation; Supervision. **Peter H. Cenijn**: Formal analysis; Investigation; Supervision. **Marja H. Lamoree**: Methodology; Project administration. **Thomas Rundberget**: Formal analysis; Methodology. **Morten Jartun**: Project administration; Investigation. **Gijs D. Breedveld**: Conceptualization; Project administration; Supervision. **Bjørn M. Jenssen**: Project administration; Supervision; Writing—review & editing. **Christopher P. Higgins**: Conceptualization; Methodology; Project administration; Supervision; Writing—review & editing. **Timo Hamers**: Conceptualization; Methodology; Project administration; Supervision; Writing—review & editing.

Data Availability Statement—Data are available through the Supporting Information. Further inquiries can be directed to the corresponding author (hakon.austad.langberg@ngi.no).

REFERENCES

Benskin, J. P., Ikonomou, M. G., Gobas, F. A. P. C., Begley, T. H., Woudneh, M. B., & Cosgrove, J. R. (2013). Biodegradation of N-ethyl perfluorooctane sulfonamido ethanol (EtFOSE) and EtFOSE-based phosphate diester (SAmPAP diester) in marine sediments. *Environmental Science & Technology*, *47*(3), 1381–1389. https://doi.org/10.1021/es304336r

Blake, B. E., Pinney, S. M., Hines, E. P., Fenton, S. E., & Ferguson, K. K. (2018). Associations between longitudinal serum perfluoroalkyl substance (PFAS) levels and measures of thyroid hormone, kidney function, and body mass index in the Fernald Community Cohort. *Environmental Pollution*, *242*, 894–904. https://doi.org/10.1016/j.envpol.2018.07.042

Cousins, I. T., Johansson, J. H., Salter, M. E., Sha, B., & Scheringer, M. (2022). Outside the safe operating space of a new planetary boundary for per- and polyfluoroalkyl substances (PFAS). *Environmental Science & Technology*, *56*(16), 11172–11179. https://doi.org/10.1021/acs.est.2c02765

Glüge, J., Scheringer, M., Cousins, I., DeWitt, J. C., Goldenman, G., Herzke, D., Lohmann, R., Ng, C., Trier, X., & Wang, Z. (2020). An overview of the uses of per- and polyfluoroalkyl substances (PFAS). *Environmental Science: Processes & Impacts*, *22*, 2345–2373. https://doi.org/10.1039/d0em00291g

Guelfo & Higgins. (2013). Subsurface transport potential of perfluoroalkyl acids at aqueous film-forming foam (AFFF)-impacted sites. *Environmental Science and Technology*, *47*(9), 4164–4171. https://doi.org/10.1021/es3048043

Hamers, T., Kortenkamp, A., Scholze, M., Molenaar, D., Cenijn, P. H., & Weiss, J. M. (2020). Transthyretin-binding activity of complex mixtures representing the composition of thyroid-hormone disrupting contaminants in house dust and human serum. *Environmental Health Perspectives*, *128*(1), 17015. https://doi.org/10.1289/EHP5911

Jonker, W., de Vries, K., Althuisius, N., van Iperen, D., Janssen, E., ten Broek, R., Houtman, C., Zwart, N., Hamers, T., Lamoree, M. H., Ooms, B., Hidding, J., Somsen, G. W., & Kool, J. (2019). Compound identification using liquid chromatography and high-resolution noncontact fraction collection with a solenoid valve. *SLAS Technology*, *24*(6), 543–555. https://doi.org/10.1177/2472630319848768

Jonkers, T. J. H., Meijer, J., Vlaanderen, J. J., Vermeulen, R. C. H., Houtman, C. J., Hamers, T., & Lamoree, M. H. (2022). High-performance data processing workflow incorporating effect-directed analysis for feature prioritization in suspect and nontarget screening. *Environmental Science & Technology*, *56*(3), 1639–1651. https://doi.org/10.1021/acs.est.1c04168

Korevaar, T. I., Muetzel, R., Medici, M., Chaker, L., Jaddoe, V. W., de Rijke, Y. B., Steegers, E. A., Visser, T. J., White, T., Tiemeier, H., & Peeters, R. P. (2016). Association of maternal thyroid function during early pregnancy with offspring IQ and brain morphology in childhood: A population-based prospective cohort study. *The Lancet Diabetes & Endocrinology*, *4*(1), 35–43. https://doi.org/10.1016/S2213-8587(15)00327-7

Landers, K., & Richard, K. (2017). Traversing barriers—How thyroid hormones pass placental, blood-brain and blood-cerebrospinal fluid barriers. *Molecular and Cellular Endocrinology*, *458*, 22–28. https://doi.org/10.1016/j.mce.2017.01.041

Langberg, H. A., Arp, H. P. H., Breedveld, G. D., Slinde, G. A., Høiseter, Å., Grønning, H. M., Jartun, M., Rundberget, T., Jenssen, B. M., & Hale, S. E. (2021). Paper product production identified as the main source of per- and polyfluoroalkyl substances (PFAS) in a Norwegian lake: Source and historic emission tracking. *Environmental Pollution*, *273*, 116259. https://doi.org/10.1016/j.envpol.2020.116259

Langberg, H. A., Breedveld, G. D., Slinde, G. A., Grønning, H. M., Høisæter, Å., Jartun, M., Rundberget, T., Jenssen, B. M., & Hale, S. E. (2020). Fluorinated precursor compounds in sediments as a source of perfluorinated alkyl acids (PFAA) to Biota. *Environmental Science & Technology*, *54*(20), 13077–13089. https://doi.org/10.1021/acs.est.0c04587

Langberg, H. A., Hale, S. E., Breedveld, G. D., Jenssen, B. M., & Jartun, M. (2022). A review of PFAS fingerprints in fish from Norwegian freshwater bodies subject to different source inputs. *Environmental Science Process & Impacts*, *24*, 330–342. https://doi.org/10.1039/d1em00408e

Liberatore, H. K., Jackson, S. R., Strynar, M. J., & Mccord, J. P. (2020). Solvent suitability for HFPO-DA ("GenX" Parent Acid) in toxicological studies. *Environmental Science & Technology Letters*, *7*(7), 477–481. https://doi.org/10.1021/acs.estlett.0c00323

McCarthy, C., Kappleman, W., & DiGuiseppi, W. (2017). Ecological considerations of per- and polyfluoroalkyl substances (PFAS). *Current Pollution Reports*, *3*(4), 289–301. https://doi.org/10.1007/s40726-017-0070-8

Nickerson, A., Maizel, A. C., Kulkarni, P. R., Adamson, D. T., Kornuc, J. J., & Higgins, C. P. (2020). Enhanced extraction of AFFF-associated PFASs from source zone soils. *Environmental Science & Technology*, *54*(8), 4952–4962. https://doi.org/10.1021/acs.est.0c00792

Nickerson, A., Rodowa, A. E., Adamson, D. T., Field, J. A., Kulkarni, P. R., Kornuc, J. J., & Higgins, C. P. (2021). Spatial trends of anionic,

zwitterionic, and cationic PFASs at an AFFF-impacted site. *Environmental Science & Technology*, *55*(1), 313–323. https://doi.org/10.1021/acs.est.0c04473

Ren, X. M., & Guo, L. H. (2012). Assessment of the binding of hydroxylated polybrominated diphenyl ethers to thyroid hormone transport proteins using a site-specific fluorescence probe. *Environmental Science & Technology*, *46*(8), 4633–4640. https://doi.org/10.1021/es2046074

Richardson, S. J. (2007). Cell and molecular biology of transthyretin and thyroid hormones. *International Review of Cytology*, *258*, 137–193.

Richardson, S. J., Wijayagunaratne, R. C., D'Souza, D. G., Darras, V. M., & Van Herck, S. L. (2015). Transport of thyroid hormones via the choroid plexus into the brain: The roles of transthyretin and thyroid hormone transmembrane transporters. *Frontiers in Neuroscience*, *9*(March), 1–8. https://doi.org/10.3389/fnins.2015.00066

Sunderland, E. M., Hu, X. C., Dassuncao, C., Tokranov, A. K., Wagner, C. C., & Allen, J. G. (2019). A review of the pathways of human exposure to poly- and perfluoroalkyl substances (PFASs) and present understanding of health effects. *Journal of Exposure Science & Environmental Epidemiology*, *29*(2), 131–147. https://doi.org/10.1038/s41370-018-0094-1

Swedish Chemicals Agency (KEMI). (2015). Occurrence and use of highly fluorinated substances and alternatives. https://www.kemi.se/en/publications/reports/2015/report-7-15-occurrence-and-use-of-highly-fluorinated-substances-and-alternatives

Taheri, M., Haghpanah, T., Meftahi, G. H., Esfahlani, M. A., Gloshan, F., Esmailpour, K., Znangiabadi, I., Masoumi-Ardakani, Y., Nouri, F., Sheibani, V., et al. (2018). Mild permanent chronic thyroid hormones insufficiency induces cognitive dysfunction in the adult male and female rats. *Journal of Applied Pharmaceutical Science*, *8*(7), 100–106. https://doi.org/10.7324/JAPS.2018.8716

Wang, Z., DeWitt, J. C., Higgins, C. P., & Cousins, I. T. (2017). A never-ending story of per-and polyfluoroalkyl substances (PFASs)? *Environmental Science & Technology*, *51*(5), 2508–2518. https://doi.org/10.1021/acs.est.6b04806

Weiss, J. M., Andersson, P. L., Lamoree, M. H., Leonards, P. E. G., van Leeuwen, S. P. J., & Hamers, T. (2009). Competitive binding of poly- and perfluorinated compounds to the thyroid hormone transport protein transthyretin. *Toxicological Sciences*, *109*(2), 206–216. https://doi.org/10.1093/toxsci/kfp055

Weiss, J. M., Andersson, P. L., Zhang, J., Simon, E., Leonards, P. E. G., Hamers, T., & Lamoree, M. H. (2015). Tracing thyroid hormone-disrupting compounds: Database compilation and structure-activity evaluation for an effect-directed analysis of sediment. *Analytical and Bioanalytical Chemistry*, *407*(19), 5625–5634. https://doi.org/10.1007/s00216-015-8736-9

Zhang, C., McElroy, A. C., Liberatore, H. K., Alexander, N. L. M., & Knappe, D. R. U. (2021). Stability of per- and polyfluoroalkyl substances in solvents relevant to environmental and toxicological analysis. *Environmental Science & Technology*, *56*, 6103–6112. https://doi.org/10.1021/acs.est.1c03979

Zhang, S., Peng, H., Mu, D., Zhao, H., & Hu, J. (2018). Simultaneous determination of (N-ethyl perfluorooctanesulfonamido ethanol)-based phosphate diester and triester and their biotransformation to perfluorooctanesulfonate in freshwater sediments. *Environmental Pollution*, *234*, 821–829. https://doi.org/10.1016/j.envpol.2017.12.021

Zwart, N., Jonker, W., Broek, R., ten de Boer, J., Somsen, G., Kool, J., Hamers, T., Houtman, C. J., & Lamoree, M. H. (2020). Identification of mutagenic and endocrine disrupting compounds in surface water and wastewater treatment plant effluents using high-resolution effect-directed analysis. *Water Research*, *168*, 115204. https://doi.org/10.1016/j.watres.2019.115204

